Interference subspace rejection in wideband CDMA:
Modes for high data-rate operation

Hansen, Henrik; Affes, Sofiene; Mermelstein, Paul

Published in:
Proceedings on IEEE Global Telecommunications Conference

Link to article, DOI:
10.1109/GLOCOM.2001.965162

Publication date:
2001

Document Version
Publisher's PDF, also known as Version of record

Interference Subspace Rejection in Wideband CDMA: Modes for High Data-Rate Operation[1]

Henrik Hansen[1], Sofiène Affes[2] and Paul Mermelstein[2]
[1]: Dept. of Telecommunication, Tech. Univ. of Denmark,
Bldg. 371, DK-2800 Lyngby, Denmark
[2]: INRS-Télécommunications, Université du Québec,
Place Bonaventure, 900, de la Gauchetière Ouest, Niveau C
Case Postale 644, Montréal, Québec, H5A 1C6, Canada

Abstract— **This paper extends our study on a multi-user receiver structure for base-station receivers with antenna arrays in multicellular systems. The receiver employs a beamforming structure with constraints that nulls the signal component in appropriate interference subspaces. Here we introduce a new mode, ISR-D (diversities), which finds and suppresses the subspace of the identified paths of all known interferers. A frame extension technique is proposed which can be applied to all available ISR modes to increase the dimensionality of the observation space and thereby avoid noise amplification as a result of subspace suppression, as well as allow asynchronous transmission. Performance differences arise between the modes due to different sensitivities to channel identification and data detection errors. For homogeneous high data-rate situations ISR-DX manifests the best performance. However, due to its reduced complexity, ISR-TRX appears to offer the best complexity-performance tradeoffs.**

I. Introduction

Most evolving third generation cellular systems employ Code-Division Multiple-Access (CDMA). In CDMA each user is assigned a unique code which allows for demodulation at the receiver when the assigned code is known. Users' codes interfere because the received signals are not orthogonal[2]. This problem is denoted Multiple-Access Interference (MAI). Receivers which attempt to exploit MAI in the demodulation are denoted multiuser receivers, unlike traditional single users receivers, e.g., the RAKE receiver [1], which treat MAI as a contribution to the white noise. Multiuser receivers are expected to play a significant role in future cellular systems.

We present a new efficient space-time multiuser receiver structure for CDMA, denoted Interference Subspace Rejection (ISR). The basic ISR framework has been defined previously [2], and various modes of operation have been introduced. Our previous paper [2] focused on mixed-power operations. Here we concentrate on high data-rate transmission in WCDMA. Our objective is to analyze the performance of ISR modes in various high data rate situations and to find the best for particular applications.

All ISR modes strive to implement the ISR beamformer, $\underline{\mathrm{W}}_n$, which satisfies the following constraints:

$$\begin{cases} \underline{\mathrm{W}}_n^H \underline{\mathrm{Y}}_{0,n}^d = 1 & \text{(distortionless signal response)} \\ \underline{\mathrm{W}}_n^H \underline{\mathrm{I}}_{TOT,n}^d = 0 & \text{(zero interference response)} \end{cases}, \quad (1)$$

where $\underline{\mathrm{Y}}_{0,n}^d$ is the desired signal response, and $\underline{\mathrm{I}}_{TOT,n}^d$ is the total interference which we strive to reject. In practice we form a beamformer with unit response toward the desired signal and null response toward an interference subspace, which spans $\underline{\mathrm{I}}_{TOT,n}$ and varies with the ISR mode used.

ISR modes differ in the way they estimate the interference subspace. For instance ISR by Realizations (ISR-R) reconstructs interfering users using Decision Feedback (DF) over consecutive symbols to form one interfering signal per interferer, and nulls are formed in the direction of all interfering users. ISR by Total Realizations (ISR-TR) sums all reconstructed interfering users to form only one interfering signal which is rejected. We consider only modes of ISR which use DF, although ISR also offers a mode which does not use DF (ISR-H, [2]).

Here we introduce a new mode, ISR-D (diversities). Instead of rejecting reconstructed users like in ISR-R, ISR-D attempts instead to reject all reconstructed diversities[3] identified for each interfering user. The dimension of the interference subspace for ISR-D is therefore high. The interference subspace rejection therefore results in significant noise enhancement [3]. To alleviate the noise enhancement, we introduce the X-option, which allows for incorporation of past data into the observation model, which in its turn means that the reconstruction of the interference is performed over many consecutive symbols. The various ISR modes are simulated in the framework provided by the spatio-temporal array-receiver STAR [4] which provides the required channel identification and uses MRC beamforming when the interferences are not yet available.

The paper is organized as follows. In Sec. II, a brief introduction to the signal model is provided. ISR-D and the X-option are presented in Sec. III. In Sec. IV we discuss ISR processing structures. Simulations and discussion are found in Sec. V. Finally, Sec. VI concludes the paper.

II. Signal Model

We provide in this section a very brief review of the signal model presented in [3], where details can be found.

After the signal received at the antenna array of M sensors is downconverted to baseband and matched-filtered by the chip forming pulse to extract the baseband image fre-

[1]The work reported here was supported by the Bell/Nortel/NSERC Industrial Research Chair in Personal Communications.

[2]Orthogonality can be obtained on the downlink when the channel is non-selective.

[3]A diversity is formed for each propagation path received at each antenna.

0-7803-7206-9/01/$17.00 © 2001 IEEE

quency, we may write this received preprocessed signal as

$$Y(t) \;=\; \sum_{u=1}^{N_u} Y^u(t) + N(t) = \sum_{u=1}^{N_u}\sum_{f=1}^{N_f} \mathcal{Y}^{u,f}(t) + N(t), \quad (2)$$

where $Y^u(t)$ is the M-dimensional signal arriving from user u, N_u is the total number of users communicating with the base, $N(t)$ is Additive White Gaussian Noise (AWGN)[4], and $\mathcal{Y}^{u,f}(t)$ decompose the signal from user u into its $N_f = MP$ diversity branches corresponding to the number of antennas, M, multiplied by the number of paths, P, arriving at each antenna in the array.

At time nT, the preprocessed signal is sampled at the chip-rate, $1/T_c$, and framed into an observation matrix with dimension $M \times (2L-1)$, then reshaped into an observation vector by concatenating the columns, to arrive at the n^{th} spatio-temporal observation vector,

$$\underline{\mathrm{Y}}_n \;=\; \sum_{u=1}^{N_u} \underline{\mathrm{Y}}_n^u + \underline{\mathrm{N}}_n = \sum_{u=1}^{N_u}\sum_{f=1}^{N_f} \underline{\mathcal{Y}}_n^{u,f} + \underline{\mathrm{N}}_n \ . \quad (3)$$

We next define each diversity as

$$\underline{\mathcal{Y}}^{u,f} = \beta_n^{u,f}\, \underline{\mathrm{w}}_n^{u,f} \ , \quad (4)$$

where $\beta_n^{u,f}$ is the total gain associated with diversity f, and $\underline{\mathrm{w}}_n^{u,f}$ derives from the modulated code,

$$w_n^{u,f}(t) = b_n^u(t-\tau_p^u(nT))\, c_n^u(t-\tau_p^u(nT))\, \underline{\mathrm{R}}_m \ , \quad (5)$$

sampled, framed and vectorized in the same manner as described previously, where $b_n^u(t)$ and $c_n^u(t)$ are the n^{th} (differentially) encoded BPSK channel bit and code, respectively, and $\underline{\mathrm{R}}_m$ is an M-dimensional vector with zeros except at the m^{th} element. Note that only every m^{th} element of $\underline{\mathrm{w}}_n^{u,f}$ is non-zero. In Eq. 5 $\tau_p^u(nT)$ is the the p^{th} path delay of user u[5].

Finally, we elaborate our notation to further decompose signals in the n^{th} observation frame, among contributions from current symbol n and neighboring symbols $n-1$ and $n+1$. To that end, we write the received preprocessed signal as

$$\begin{aligned}\underline{\mathrm{Y}}_n &= \sum_{u=1}^{N_u} \underline{\mathrm{Y}}_n^u + \underline{\mathrm{N}}_n = \sum_{u=1}^{N_u}\sum_{f=1}^{N_f} \underline{\mathcal{Y}}_n^{u,f} + \underline{\mathrm{N}}_n \ , \quad (6)\\ &= \sum_{u=1}^{N_u}\sum_{f=1}^{N_f} \left(\underline{\mathcal{Y}}_{0,n}^{u,f} s_n^u + \underline{\mathcal{Y}}_{-1,n}^{u,f} s_{n-1}^u + \underline{\mathcal{Y}}_{+1,n}^{u,f} s_{n+1}^u \right) + \underline{\mathrm{N}}_n \ ,\end{aligned}$$

where $s_n^u = b_n^u \psi_n^u$ is the n^{th} signal component, $(\psi_n^u)^2$ being the power and b_n^u the channel bit, $\underline{\mathcal{Y}}_{0,n}^{u,f}$ is channel response of diversity f; whereas $\underline{\mathcal{Y}}_{\pm 1,n}^{u,f}$ arrives from neighboring symbols in the frame.

III. ISR-D mode and Extension to Past Data

A block diagram of ISR-D implemented with the Spatio-Temporal Array-Receiver (STAR) [4] is shown in Fig. 1. We let the desired signal be denoted by $\underline{\mathrm{Y}}_{0,n}^d s_n^d$ say $d = \{u | u = 1\}$; whereas we use the notation $\underline{\mathcal{I}}_n^{i,f} = \underline{\mathcal{Y}}_n^{i+1,f}$, $i = \{u-1 | u = 2, \cdots, N_u\}$ for other interfering users, and $\underline{\mathcal{I}}_{ISI,n}^{d,f} = \underline{\mathcal{Y}}_{-1,n}^{d,f} + \underline{\mathcal{Y}}_{+1,n}^{d,f}$ is InterSymbol Interference (ISI). The received preprocessed signal (Eq. 2) can be written as

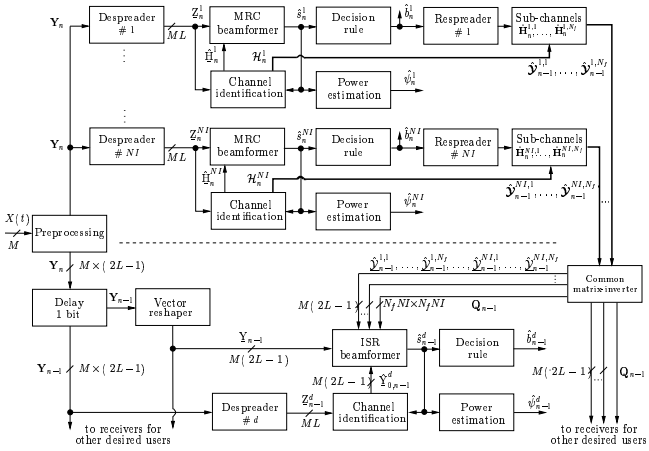

Fig. 1. Block Diagram of STAR with ISR implemented in the D mode.

$$\underline{\mathrm{Y}}_n = \underline{\mathrm{Y}}_{0,n}^d s_n^d + \sum_{f=1}^{N_f} \underline{\mathcal{I}}_{ISI,n}^{d,f} + \sum_{i=1}^{NI}\sum_{f=1}^{N_f} \underline{\mathcal{I}}_n^{i,f} + \underline{\mathrm{N}}_n \ , \quad (7)$$

where $NI = N_u - 1$ is the total number of interfering users. The ISR-D beamformer satisfies the following constraints (compare with Eq. 1)

$$\begin{cases} \underline{\mathrm{W}}_n^H \underline{\mathrm{Y}}_{0,n}^d = 1 & \text{(unit signal response)} \\ \underline{\mathrm{W}}_n^H \hat{\underline{\mathcal{I}}}_n^{i,f} = 0 & \text{(null MAI)} \\ \underline{\mathrm{W}}_n^H \hat{\underline{\mathcal{I}}}_{ISI,n}^{d,f} = 0 & \text{(null ISI)} \end{cases} . \quad (8)$$

For simplicity, we disregard in the following ISI rejection which can be implemented similarly (see also [3]). The matrix of null-constraints therefore takes the form

$$\hat{\mathbf{C}}_n = \left[\frac{\hat{\underline{\mathcal{I}}}_n^{1,1}}{\|\hat{\underline{\mathcal{I}}}_n^{1,1}\|}, \cdots, \frac{\hat{\underline{\mathcal{I}}}_n^{1,N_f}}{\|\hat{\underline{\mathcal{I}}}_n^{1,N_f}\|}, \frac{\hat{\underline{\mathcal{I}}}_n^{2,1}}{\|\hat{\underline{\mathcal{I}}}_n^{2,1}\|}, \cdots, \frac{\hat{\underline{\mathcal{I}}}_n^{NI,N_f}}{\|\hat{\underline{\mathcal{I}}}_n^{NI,N_f}\|} \right] . \quad (9)$$

Unlike with ISR-R [2], in the ISR-D operation nulling of diversities results in robustness to estimation errors in channel-path gains. We consider therefore the simpler constraint matrix (Eq. 5)

$$\hat{\mathbf{C}}_n = \left[\frac{\hat{\underline{\mathrm{w}}}_n^{1,1}}{\|\hat{\underline{\mathrm{w}}}_n^{1,1}\|}, \cdots, \frac{\hat{\underline{\mathrm{w}}}_n^{1,N_f}}{\|\hat{\underline{\mathrm{w}}}_n^{1,N_f}\|}, \frac{\hat{\underline{\mathrm{w}}}_n^{2,1}}{\|\hat{\underline{\mathrm{w}}}_n^{2,1}\|}, \cdots, \frac{\hat{\underline{\mathrm{w}}}_n^{NI,N_c}}{\|\hat{\underline{\mathrm{w}}}_n^{NI,N_c}\|} \right] , \quad (10)$$

whose components hold codes modulated by estimated symbols. The ISR-D beamformer is then computed from

$$\mathbf{Q}_n \;=\; \left(\hat{\mathbf{C}}_n{}^H \hat{\mathbf{C}}_n \right)^{-1} \ , \quad (11)$$

$$\mathbf{\Pi}_n \;=\; \mathbf{I}_{M(2L-1)} - \hat{\mathbf{C}}_n \mathbf{Q}_n \hat{\mathbf{C}}_n{}^H \ , \quad (12)$$

$$\underline{\mathrm{W}}_n^d \;=\; \frac{\mathbf{\Pi}_n \hat{\underline{\mathrm{Y}}}_{0,n}^d}{\hat{\underline{\mathrm{Y}}}_{0,n}^{d\ H} \mathbf{\Pi}_n \hat{\underline{\mathrm{Y}}}_{0,n}^d} \ , \quad (13)$$

where $\mathbf{I}_{M(2L-1)}$ is the $M(2L-1)$-dimensional identity matrix. When $M > 1$, $\left(\hat{\mathbf{C}}_n^H \hat{\mathbf{C}}_n \right)^{-1}$ has dimension $MPN_u \times$

[4]Other users unknown to the base, thermal noise etc.

[5]Note that we could as well write $\tau^{u,f}(nT)$, however, it is assumed that each propagation path arrives simultaneously at all antennas, and therefore this notation is used.

MPN_u. However, the matrix is sparse because $\hat{\underline{w}}_n^{u,f}$ is non-zero only at elements $m, m+M,\ m+2M,\ \cdots,\ m+(2L-1)M$; and the matrix inversion boils down to M inversions of a $PN_u \times PN_u$ dimensional matrix. Given the ISR-D beamformer, the ISR-D signal estimate is found as $\hat{s}_n = \Re\left\{ \underline{W}_n^{d\,H} \underline{Y}_n \right\}$ and for the particular case of BPSK signaling, the BPSK channel bit estimate becomes $\hat{b}_n = \text{sign}\{\hat{s}_n\}$.

Note that the signal $\underline{Y}_n$ in Eq. 6 can be formulated as

$$\underline{Y}_n = \left[\underline{w}_n^{1,1}, \cdots, \underline{w}_n^{N_u,N_f}\right] \begin{bmatrix} \beta_n^{1,1} \\ \vdots \\ \beta_n^{N_u,N_f} \end{bmatrix} + \underline{N}_n = \mathbf{C}_n\, \underline{\beta}_n + \underline{N}_n.$$

The estimation of $\underline{\beta}_n$ (i.e., the channel coefficients of the N_u users) may be regarded as a multi-source problem [5]:

$$\hat{\underline{\beta}}_n^{ms} \quad = \quad \mathbf{F}_n^H \underline{Y}_n = \mathbf{Q}_n \mathbf{C}_n^H \underline{Y}_n\ , \tag{14}$$

which is just one step in the estimation of the ISR-D signal estimate (Eqs. 12 and 13) when the estimate $\hat{\mathbf{C}}_n$ replaces $\mathbf{C}_n$. Computing $\hat{\underline{\beta}}_n^{ms}$ in the D mode allows joint signal combining and channel estimation.

When the number of users becomes high compared to the processing gain, the dimension of the interference subspace becomes comparable to the total observation dimension $N_T = M(2L-1)$. Unlike ISR-TR [2], which always requires one constraint only, ISR-R [2] and ISR-D may suffer a large degradation because the number of constraints required becomes comparable to the total dimension available. An ISR option, which is denoted the X-option (e.g., ISR-DX) mitigates this by introducing additional data from previously transmitted symbols into the observation frame and hence increase dimensionality. This option is described in detail in [3].

IV. ISR Processing Structures

A. Joint ISR Detection

Previously we focused on a selective implementation of ISR, where ISR is applied to a selected group of users, typically users with a low data rate, who strive to suppress interference generated by a selected group of high rate users. Although this approach is appropriate when the number of HR users is very low, mutual interference suppression among HR users may be desired as well, because the interference caused by other HR users may be significant. Therefore, in this section we introduce joint ISR detection. In joint ISR, we modify the projector of Eq. 12 to the following form,

$$\mathbf{\Pi}_n^d = \mathbf{I}_{N_T} - \hat{\mathbf{C}}_n \mathbf{Q}_n \hat{\mathbf{C}}_n^{d\,H}, \tag{15}$$

where the columns of $\hat{\mathbf{C}}_n$ now span all users communicating with the base, whereas $\hat{\mathbf{C}}_n^d$ is the user specific signal blocking matrix belonging to the desired user, which we index by superscript d. Note that the projection matrix now becomes user specific. The beamformer is computed as usual by using Eq. 15 instead of Eq. 12. Details can be found in [3].

B. Successive versus Parallel Detection

It is already documented in literature that successive IC may sometimes outperforms parallel IC. For instance, SIC and PIC are compared to conclude that SIC outperforms PIC in adverse power control situations; whereas PIC outperforms SIC when power control is perfect [6], [7]. Also, the decorrelating decision feedback algorithm [8], [9] uses a successive structure. In a first stage the signal is whitened, then DF is used successively in the second stage, and processing is continued in order of decreasing interferer power.

The successive approach generalizes readily to ISR. Suppose that N_u users are ranked in order of decreasing received power. Processing user j, we therefore reconstruct users $1,\ \cdots,\ j-1$ and sum them to form the constraint matrix of null constraints. Then the n^{th} ISR symbol estimate of user j is computed and the estimate is used for the processing of remaining users $j+1,\ \cdots,\ N_u$. For details regarding successive ISR processing refer to [3].

C. Multistage Processing: M-option

The DF modes of ISR (TR,R,D) use coarse Maximal Ratio Combined (MRC) symbol estimates at a preliminary stage in order to reconstruct signals for the ISR operation. MRC estimates are less reliable than ISR estimates causing worse reconstruction errors. Using improved ISR estimates to reconstruct the interferences and repeat the ISR operation in successive stages can provide better results. We denote this possibility the M-option. Details can be found in [3].

V. Simulations and Discussion

In this section we provide simulation results to compare and analyze the performance of the various ISR modes. For comparison we consider also the SIC and the PIC. We summarize our results and discuss the applications of modes.

A. Simulation Setup

We consider the uplink of a differentially encoded BPSK DS-CDMA with chip rate $R_c = 4.096$ Mcps operating at a carrier of $f_c = 1.9$ GHz. The processing gain, defined as the ratio between the chip rate and the channel bit rate, is fixed to $L = 16$ (i.e., 256 Kbps). N_u users communicate with the base-station and users from other sectors/cells along with thermal noise are modeled as Additive White Gaussian Noise (AWGN). The channel is considered Rayleigh fading [10] with Doppler frequency f_D, and we consider frequency-selective fading with $P = 3$ propagation paths having relative strengths 0 dB, - 6dB, -10 dB. Delays are random but inter-path delays are greater than one chip. The base-station receiver is equipped with M antennas. We implement closed loop power control operating at 1600 Hz and adjusting the power in steps of ± 0.5 dB. A simulated error rate on the power control bit of $\text{BER}_{\text{PC}} = 10\%$ is used. Channel estimates obtained by STAR [4] are used for all modes including SIC and PIC but joint combining and channel estimation is used for the D-mode (Sec. III).

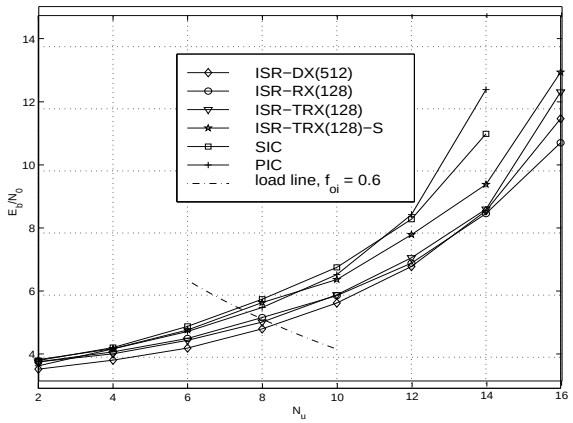

Fig. 2. Single antenna.

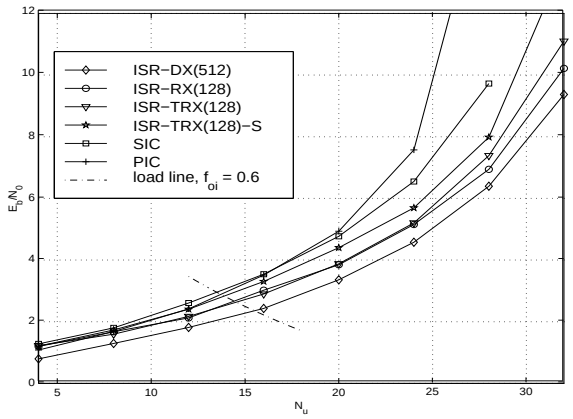

Fig. 3. Two antennas.

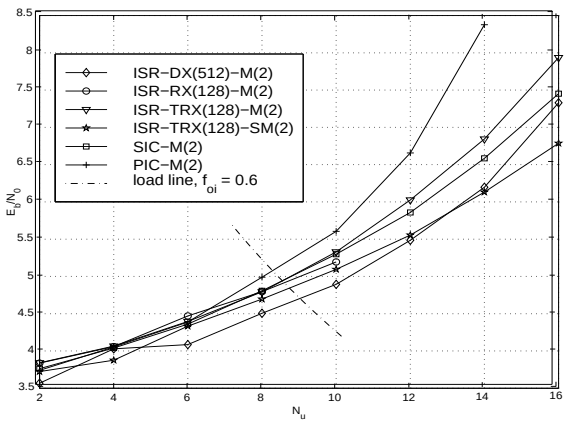

Fig. 4. Multistage ISR processing.

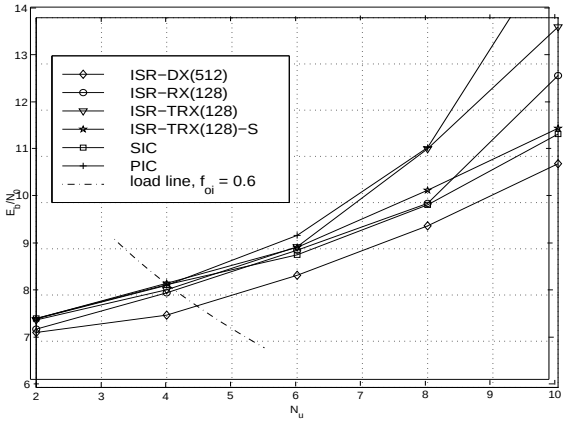

Fig. 5. ISR in high Doppler and $M = 2$ antennas.

B. Simulation Results

First we consider the slow Doppler situation with $f_D = 9$ Hz[6] and $M = 1$ receiving antenna. Fig. 2 depicts the E_b/N_0 required to obtain BER of 5%[7] with different number of users obtained by search. The figure shows performance curves for various modes of ISR; SIC and PIC performances are shown for comparison. Numbers in braces denote the temporal dimension employed (X-option). The system setup is the same as in the previous section. All DF ISR modes provide roughly the same performance ($N_u \leq 14$), but better than subtractive receivers, particularly when the system load is high. The successive implementation of ISR-TRX, ISR-TRX-S, provides slightly worse performance than its parallel version, but better than SIC[8]. ISR-TRX-S and SIC are similar up to the point of interference rejection; ISR-TRX-S nulls interference, whereas SIC subtracts it. ISR-TRX-S therefore gains robustness compared to SIC by virtue of its higher robustness to estimation errors, especially to power estimation errors.

The load line dictates the operating condition when all in-cell interference is suppressed, while neighboring cells are assumed to have same load as the target cell and when the out-cell to in-cell interference ratio is $f_{oi} = 0.6$ [1]. Capacities range from 7 users for SIC and PIC to 8 users for ISR-DX which achieves the best performance. Other ISR modes perform slightly worse that ISR-DX but better than the subtractive receivers. These capacities may be exceeded if out-cell interferers are suppressed as well, or if the cell is isolated.

Fig. 3 shows performance with $M = 2$ antennas. Generally, all methods gain in performance by the same amount. Required E_b/N_0 is about 3 dB lower and the number of users accommodated is almost doubled. This increase is not surprising, since noise is now distributed over two receiving antennas (antenna gain) and the dimensionality is doubled. Furthermore, variations of received powers are reduced because the number of diversities $N_f = MP$ is doubled. ISR-DX offers slightly better performance than other DF modes because the E_b/N_0 working point is generally 3 dB lower where the identification of the channel is actually worse. This tends to favor ISR-DX which is completely insensitive to estimation errors of the channel gain. Again, ISR-TRX-S outperforms SIC. The load line suggests that at the low end 13 users can be supported with PIC but ISR-DX may serve about 15 users. Doubling the number of antennas, therefore, increases capacity by a factor of about 1.8.

Fig. 4 provides performance curves with $M = 1$ antenna when the number of ISR stages is increased to two. Com-

[6]Corresponding to a mobile speed of 5 Kmph.

[7]A BER of 5% is considered applicable to WCDMA [11], [12] before channel decoding.

[8]The SIC relates to the PIC like ISR-TRX-S relates to ISR-TRX

paring these with the one-stage curves of Fig. 2, the performance of all modes is improved by about 0.5 dB near $N_u = 8$. This improvement increases to about 5 dB for ISR-TRX at $N_u = 16$. This confirms that DF based on MRC estimates for one-stage operation is good when interference noise is low (low or moderate number of users) but becomes degraded when MAI is significant (high N_u). SIC-M and ISR-TRX-SM achieve performance comparable to multistage ISR, except ISR-DX-M. ISR-TRX-SM is, however, better than SIC-M and has performance close to ISR-DX-M and even outperforms it at very high loads.

In Fig. 5 we use again $M = 2$ antennas but increase the Doppler speed to 180 Hz reflecting mobile speeds of 100 Kmph. Compared with the low Doppler situation in Fig. 3, all modes are seen to suffer from increased Doppler because power control is not able to follow variations of the channel, causing greater power fluctuations and worse identification of the channel. This is seen to favor ISR-DX (relative to other modes) which promises the best robustness to channel identification errors. Again ISR generally outperforms subtractive receivers. The load line shows that capacity is reduced to 10 (PIC) and 12 (ISR-DX); that is, a reduction about 25%. Practical systems are dominated by users with low mobility and therefore this capacity reduction is no significant.

C. Discussion

Generally, all ISR modes of operation outperform receivers with interference cancellation by subtraction (SIC and PIC). Only with multistage processing is SIC able to take sufficient advantage of successive processing of users to outperform ISR-TRX,RX; but not ISR-DX. However, the ISR alternative to SIC, ISR-TRX-S provides generally better performance, underlining the effectiveness of linearly constrained subspace suppression as opposed to interference subtraction. Differences between ISR modes are not significant and become evident in adverse situations only (e.g., high Doppler).

The DF modes rank in performance as ISR-DX > ISR-RX > ISR-TRX [3], which is also the exact ranking of complexity. Therefore, ISR-TRX with same complexity as the PIC (see [3]) is a very attractive solution in most situations as it combines affordable complexity with satisfactory performance. A more detailed complexity assessment [3] shows that further improvements in performance may be obtained at the least cost in complexity by increasing the number of processing stages (ISR-TRX-M) rather than using more advanced modes.

VI. Conclusions

This paper presented a new ISR mode of operation, ISR by Diversities (ISR-D). ISR-D uses the finest decomposition of interference among DF modes of operation, and strives to reject all interfering diversities. ISR-D is the mode most robust to channel identification errors, but is also the most expensive solution computationally. Several new processing structures including past data extension (X-option), joint ISR detection and multistage (M-option) were also introduced.

The DF modes of ISR are analyzed by simulations. ISR-TRX provides generally very good performance in most situations when identification is good. Moreover, it always outperforms PIC and generally outperforms SIC, both of which possess the same level of complexity. ISR-TRX is therefore a very attractive solution. ISR offers also a successive formulation, ISR-TRX-S. It shows its power (compared to ISR-TRX) in high Doppler, and it always outperforms the SIC. However, it inherits the pronounced processing delay of SIC, which makes its implementation difficult. Although advanced modes (R,D) outperform ISR-TRX, their use is warranted only in adverse situations, such as high Doppler, where channel identification is poor. However, if it can be assumed that the low Doppler situation is predominant, it is better to use ISR-TR with more stages (ISR-TRX-M), instead of the more elaborate modes (R,D).

Interference subspace rejection with STAR, STAR-ISR, achieves significant improvements in the uplink data-transmission capacity of multicellular CDMA networks.

References

[1] A. J. Viterbi, *CDMA Principles of Spread Spectrum Communication*, vol. 1 of *Addison-Wesley Wireless Communication Series*, Addison-Wesley, 1997.

[2] S. Affes, H. Hansen, and P. Mermelstein, "Interference subspace rejection in wideband CDMA: Modes for mixed-power operation," *ICC'01*, vol. 2, pp. 523–529, 2001.

[3] S. Affes, H. Hansen, and P. Mermelstein, "Interference subspace rejection: a framework for multiuser detection in wideband CDMA," *Submitted to IEEE Journal on Selected Areas in Communications, October 2000, revised August 2001, in review.*

[4] S. Affes and P. Mermelstein, "A new receiver structure for asynchronous CDMA: STAR - the spatio-temporal array receiver," *IEEE J. on Selected Areas in Communications.*, vol. 16, no. 8, pp. 1411–1422, October 1998.

[5] S.Affes, S. Gazor, and Y. Grenier, "An algorithm for multi-source beamforming and multi-target tracking: Further results," *Proceedings of EUSIPCO-96*, vol. 1, pp. 543–546, 1996.

[6] P. Patel and J. Holtzman, "Performance comparison of a DS/CDMA system using a successive interference cancellation (IC) scheme and a parallel IC scheme under fading," *Proc. ICC'94, New Orleans, LA*, pp. 510–514, May 1994.

[7] S. H. Hwang, C. G. Kang, and S. W. Kim, "Performance analysis of interference cancellation schemes for a DS/CDMA system under delay constraints," *PIMRC'96*, pp. 569 –573, 1996.

[8] A. Duel-Hallen, "Decorrelating decision-feedback multiuser detector for synchronous code-division multiple access channels," *IEEE Trans. on Communication*, vol. 41, pp. 285–290, Feb. 1993.

[9] A. Duel-Hallen, "A family of decision-feedback detectors for asynchronous code-division multilple-access channels," *IEEE Trans. on Communication*, vol. 43, no. 2/3/4, pp. 421–343, February/March/April 1995.

[10] Ed. W. C. Jakes, *Microwave Mobile Communications*, John Wiley & Sons, 1974.

[11] F. Adachi, M. Sawahashi, and H. Suda, "Wideband DS-CDMA for next generation mobile communications systems," *IEEE Communications Magazine*, vol. 9, no. 36, pp. 55–69, Sep. 1998.

[12] R. Prasad, "An overview of CDMA evolution toward wideband CDMA," *IEEE Communications Surveys*, vol. 1, no. 1, pp. 2–29, Fourth Quarter 1998.